Response Statement to Community's Comments (CC3)

Wang and Jeng

January 24, 2026

The authors thank the reviewer for the valuable comments. The manuscript has been revised by carefully considering all the comments. The changes are highlighted in the marked copy, and detailed responses to the reviewer's comments are provided below.

Comment #CC3:

You have two verification benchmarks, but the paper itself acknowledges no lab/field quantitative validation. While this isnt a fatal flaw, you do need to strengthen credibility with additional numerical evidence. Consider adding (1) Grid/time-step sensitivity for one representative case (even a coarse/medium/fine study + one plot at the monitoring point). (2) Splitting / sub-stepping sensitivity: show that results don't materially change when the chemistry sub-step size changes within a window (or quantify the trade-off). Your own text highlights synchronisation issues, so you should demonstrate control. (3) For benchmark 2, quantify mismatch: e.g., L2 error vs time, and show it decreases with refinement or explain the irreducible discrepancy (boundary formulation differences are mentioned but not demonstrated).

Response:

We thank the reviewer for this constructive comment and for the specific suggestions on strengthening the numerical credibility of the framework in the absence of laboratory or field-scale validation.

In response, we have augmented the manuscript with additional numerical evidence addressing points (1)–(3) as follows. First, a grid and time-step sensitivity analysis has been added for a representative test case, using coarse, medium, and fine discretisations. The results are evaluated at a monitoring location and demonstrate that the key hydro-mechanical and chemical responses are insensitive to further refinement within the investigated resolution range.

Second, we have extended the splitting and chemistry sub-stepping sensitivity analysis to explicitly demonstrate that the results remain stable when the chemical sub-step size is varied within a prescribed window. This

directly addresses the synchronisation and operator-splitting considerations highlighted in the manuscript and confirms that the adopted coupling strategy is numerically controlled.

Third, for Benchmark #2, the discrepancy is dominated by differences in the advective transport formulation: the benchmark employs a conservative face-based volumetric flux, whereas the present framework represents advection through the divergence of a Darcy-based, cell-centred flux under near-saturated conditions. These formulations are not equivalent at the discrete level, and therefore a non-zero irreducible mismatch remains even under mesh and time-step refinement.

Taken together, the added sensitivity analyses and quantitative error assessment demonstrate that the present implementation is numerically stable, well controlled with respect to discretisation and splitting choices, and that the observed benchmark discrepancy reflects structural differences between the governing formulations rather than numerical inconsistency.

[Deleted content:] ~~The simulated concentration profiles of dissolved Ca were compared with those of the reference study, as illustrated in Figure. These two solutions agree well at intermediate and late times, but noticeable deviations appear in the early stage of the breakthrough. These differences arise primarily from variations in the underlying transport formulations and boundary representations. The present solver accounts for near-saturation effects, which modify the advective flux through compressibility terms, whereas the reference benchmark adopted a classical ADE-based formulation with constant porosity and a prescribed uniform flow field. As the dissolution front advanced and concentration gradients became less steep, the two solutions gradually converged, although a small residual discrepancy persisted because of the fundamentally different governing equations and kinetic parameterisations.~~

[Added new content:] *Within the OpenFOAM framework adopted in this study, the governing equations were discretised using the finite volume method. Diffusive and dispersive fluxes were evaluated using the Gauss linear scheme, while the advective term of solute transport was discretised using a Gauss limitedLinear scheme with a limiter coefficient of 1 in order to suppress spurious oscillations. Temporal integration was performed using the implicit Euler method. The pressure, displacement and concentration equations were solved using the GAMG solver with a DILU preconditioner, with absolute and relative tolerances of* 10^{-9} *and zero, respectively. The coupled HMC system was advanced using a segregated outer-iteration strategy, and convergence was achieved when the residuals of all primary variables dropped below* 10^{-6}*. Further implementation details are provided in the companion paper (Wang and Jeng, 2025).*

To strengthen the numerical credibility of the proposed HMC framework, a systematic sensitivity analysis was conducted with respect to spatial discretisation, global time-step size and chemical sub-stepping in the ChemWindow controller. A one-at-a-time strategy was adopted, whereby only one numerical factor was varied while all others were kept identical.

The numerical deviations were quantified using the mean relative error (MRE) and maximum relative error (MaxRE), defined as

$$MRE = \frac{1}{N}\sum_{i=1}^{N}\left|\frac{y_i - y_i^{\mathrm{ref}}}{y_i^{\mathrm{ref}}}\right|, \quad MaxRE = \max_{1\le i\le N}\left|\frac{y_i - y_i^{\mathrm{ref}}}{y_i^{\mathrm{ref}}}\right|, \tag{1}$$

where y_i denotes the computed value at the i-th comparison point and y_i^{ref} is the corresponding value obtained from the finest reference solution. The MRE reflects the overall deviation level, whereas the MaxRE captures the largest local discrepancy associated with potential non-linear or synchronisation effects.

The reference configuration corresponds to the finest grid ($120 \times 1 \times 100$), the smallest global time step ($\Delta t = 1.58 \times 10^5$ s), and the smallest chemical sub-step ($\Delta t_c = 3000$ s). The medium discretisation employs a grid of $60 \times 1 \times 50$ with $\Delta t = 3.15 \times 10^5$ s and $\Delta t_c = 6000$ s, while the coarse setting uses $30 \times 1 \times 25$, $\Delta t = 6.31 \times 10^5$ s, and $\Delta t_c = 12000$ s.

Table 1: Grid-, time-step-, and chemical-substep-independence summary.

Variable	**Grid mean (%)**	**Grid max (%)**	**Time-step mean (%)**	**Time-step max (%)**	**Chem. sub-step mean (%)**	**Chem. sub-step max (%)**
p	$1.2 \rightarrow 0.43$	$1.9 \rightarrow 0.45$	$0.25 \rightarrow 0.08$	$0.27 \rightarrow 0.09$	–	–
$\mathbf{u}_s$	$0.54 \rightarrow 0.07$	$0.92 \rightarrow 0.11$	$0.76 \rightarrow 0.25$	$0.77 \rightarrow 0.26$	–	–
Y.C	$5.5 \rightarrow 2.1$	$11.5 \rightarrow 3.8$	$0.15 \rightarrow 0.05$	$0.35 \rightarrow 0.11$	$0.7 \rightarrow 0.4$	$1.1 \rightarrow 0.6$

Table 1 together with Figs. 1 and 2 summarises the grid-, time-step- and chemical-substep-independence results for pore pressure p, solid displacement $\mathbf{u}_s$ and solute concentration Y.C. For the hydro-mechanical variables p and $\mathbf{u}_s$, both the MRE and MaxRE decrease rapidly with mesh refinement and global time-step reduction. In all medium–fine comparisons, the maximum relative errors remain below 0.5%, indicating excellent numerical convergence of the hydro-mechanical part of the solver.

The solute concentration Y.C exhibits a higher sensitivity to spatial resolution, as expected for advection–dispersion–reaction dominated processes. Nevertheless, the MaxRE decreases from 11.5% in the coarse–fine comparison to 3.8% in the medium–fine comparison, while the MRE reduces from 5.5% to 2.1%, demonstrating satisfactory convergence of the transport component. In contrast, the sensitivity to the global time-step size is negligible, with maximum discrepancies below 0.2%. More importantly, decreasing the chemical sub-step size from 12,000 s to 3,000 s results in less than 1% variation in solute concentration, with the MaxRE reducing from 1.1% to 0.6%. This confirms that the proposed ChemWindow synchronisation scheme is numerically stable and does not introduce artificial splitting errors.

Based on these results, the medium discretisation settings ($60 \times 1 \times 50$, $\Delta t = 3.15 \times 10^5$ s, $\Delta t_c = 6000$ s) are adopted in the remainder of this study as a balanced compromise between numerical accuracy and computational

efficiency.

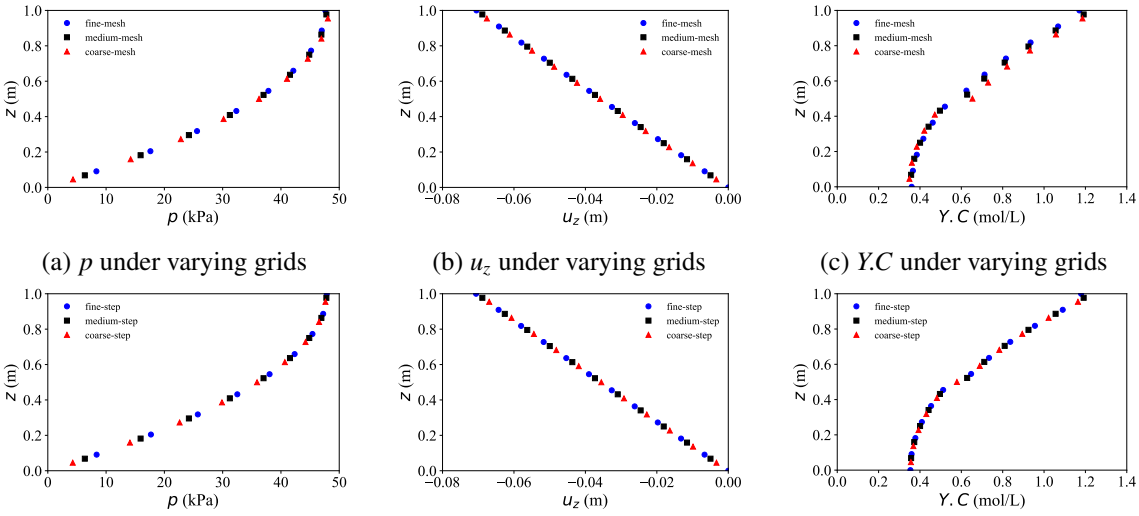

(a) p under varying grids (b) u_z under varying grids (c) $Y.C$ under varying grids

(d) p under varying time steps (e) u_z under varying time steps (f) $Y.C$ under varying time steps

Figure 1: Analysis of grid and time step independence: Fine grid and small time step (round), medium grid and step (square), coarse grid and large step (triangle).

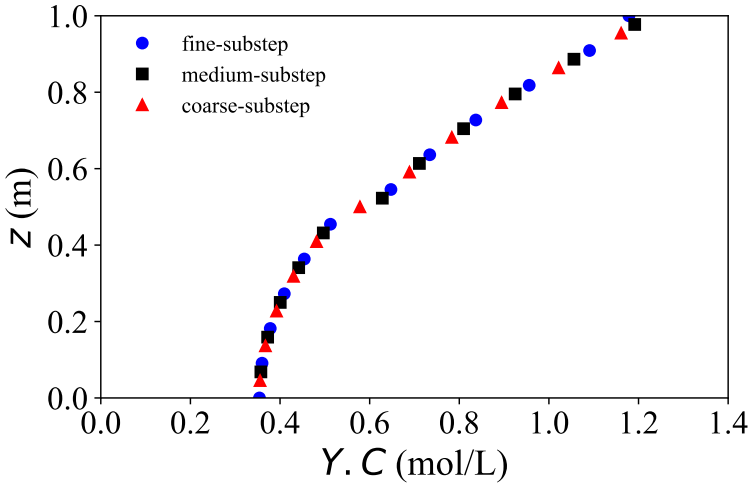

Figure 2: Analysis of chemical-substep independence: small substep (round), medium substep (square), large substep (triangle).

[Line 323–339]

The simulated concentration profiles of dissolved Ca were compared with those reported in the reference study, as shown in Fig. Overall, the two solutions exhibit good agreement at intermediate and late times, whereas noticeable discrepancies arise during the early breakthrough stage.

The discrepancies observed between the two solutions are primarily attributed to the fundamentally different discrete treatments of the advective transport term, which lead to distinct boundary flux reconstructions. The

reference solver evaluates the advective operator using the surface-based volumetric flux field ϕ in the form $\nabla\cdot(\phi Y_i)$, whereas the present framework formulates advection in terms of the divergence of a Darcy-based, cell-centred mass flux, $\nabla\cdot(\mathbf{v_f} Y_i)$. Owing to the distinct surface-flux and volume-flux formulations, the two operators are not discretely equivalent.

Consequently, even when identical fixedValue boundary conditions are prescribed, the resulting advective fluxes differ in the discrete implementation, because ϕ is imposed directly at cell faces, while $\mathbf{v_f}$ is defined at cell centres and subsequently interpolated to the boundary faces. This structural difference cannot be expected to vanish systematically through mesh refinement and therefore gives rise to irreducible discrepancies during the early transient stage.

Within this context, Benchmark #2 is not intended to provide strict equation-to-equation validation against the reference solution, but rather to assess the correctness and feasibility of the proposed governing equations under comparable conditions. The observed agreement in the overall trend and magnitude of the concentration profiles supports the correctness of the present implementation and indicates that the proposed control equations capture the dominant dissolution dynamics. The remaining differences are mainly attributable to the distinct discrete treatments of the advective operator.

[Line 323–339]

References

Wang, B.L., Jeng, D.S., 2025. Three-dimensional model for consolidation-induced solute transport in a nearly saturated porous medium. International Journal for Numerical and Analytical Methods in Geomechanics 49, 4436–4464. doi:https://doi.org/10.1002/nag.70070.